Implementation of Channel Estimation for MIMO-OFDM Systems

Chih-Hung Lin, Robert Chen-Hao Chang, *Senior Member*, *IEEE*, Kuang-Hao Lin*, and Yang-Yu Lin
Department of Electrical Engineering, National Chung Hsing University, Taichung, Taiwan
*Department of Electronic Engineering, National Chin-Yi University of Technology, Taichung, Taiwan
holin@nchu.edu.tw; khlin@ncut.edu.tw; chchang@dragon.nchu.edu.tw

***Abstract*—In modern Wireless Local Area Network (WLAN), both the transmitting data throughput and the connecting stability are very important. For the IEEE802.11n protocol specification, it is made of a multi-input multi-output (MIMO) system and an Orthogonal Frequency Division Multiplexing (OFDM) system. In order to decrease the decoding error rate at the receiving end and to fully restore the original transmitting signal, estimation of the channel response information is necessary. In this paper, a combined channel estimation algorithm is proposed by using TDT-L-STBC, which can increase the MIMO channel estimation performance. The proposed architecture of MIMO-2x2 is implemented and verified by TSMC 0.18 µm CMOS technology.**

Index Terms—*Channel estimation, MIMO, OFDM.*

I. INTRODUCTION

A recent surge of research on wireless local area networks (WLANs) has generated new challenges and opportunities. With the increasing usage of wireless communication systems, reliability requirements for high data rates have become more critical. In view of this, the IEEE 802.11n system is based on multiple input multiple output (MIMO)-orthogonal frequency division multiplexing (OFDM) technology. The advantages of MIMO-OFDM are that it uses bandwidth more efficiently, and combats the inter-symbol interference (ISI) effect and multi-path effect. Therefore, it is the current trend in WLAN development is to use MIMO-OFDM technology [1], [2].

In MIMO-OFDM systems, the information in the channel matrix is essential for decoding the transmitted message correctly. If the channel matrix is not estimated accurately, the channels cannot be fully decoupled at the receiver and the spatial streams become coupled. This paper proposed a combined channel estimation algorithm. With the transformation of frequency domain – time domain and the very low sub-carrier channel impulse response interference in time-domain, we can get the upper limit of the sub-carrier with channel impulse response, *L*. Transforming back the channel impulse response that we wanted, combining with space time block code (STBC) [3], [4] and adding the correction of the preamble symbol and the noise, its bit error rate (BER) will be decreased to a certain level. Compared with the conventional channel estimation algorithm, it consumes a little more hardware area but the performance is increased.

This paper is organized as follows. The system block diagram of the MIMO-OFDM baseband receiver is described in Section II. The channel estimation algorithms are presented in Section III. Simulation results are shown in Section IV. Implementation results are given in Section V. Finally, Section VI concludes this investigation.

II. SYSTEM BLOCK DIAGRAM

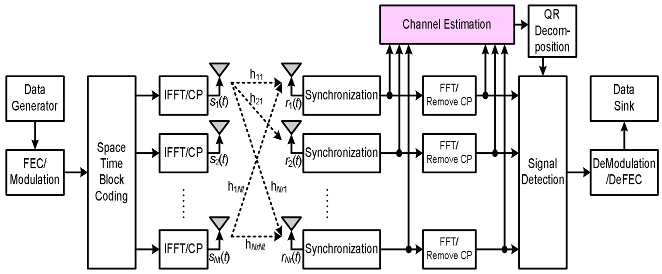

Figure 1. The structure of STBC channel estimation and signal detection in MIMO-OFDM system

Fig. 1 includes the transmitting and receiving ends of OFDM system. The source data pass through a modulator, inverse fast Fourier transform (IFFT) and DAC to reach the transmitting antennas of the transmitter. After passing through the channel, additive white Gaussian noise (AWGN) is added. Then, the signal will be received and converted to digital with an ADC in the receiver and by fast Fourier transform (FFT), since the signals contain noise, the channel frequency response can be obtained according to the pilot signals and their positions.

In Fig. 1, the spatial multiplex is used in the MIMO system with *Mt* transmitted and *Mr* received antennas. The baseband equivalent model can be described as:

$$\boldsymbol{R} = \boldsymbol{HS} + \boldsymbol{N} \tag{1}$$

where $\boldsymbol{R}$, $\boldsymbol{H}$, $\boldsymbol{S}$, $\boldsymbol{N}$ represent received signals matrix, channel matrix, transmitted data matrix, and noise matrix. The transmitting data $\boldsymbol{S}$ becomes *Mt* sub-carriers after passing through space-time encoder. By the channel message system between the transmitting and the receiving antennas, the receiving end receives *Mr* sub-carriers, and with the space-time decoding, data $\boldsymbol{R}$ is obtained. The channel response matrix $\boldsymbol{H}$ can be expressed as:

$$\boldsymbol{H} = \begin{bmatrix} h(1,1) & \cdots & h(1,Mt) \\ \vdots & \ddots & \vdots \\ h(Mr,1) & \cdots & h(Mr,Mt) \end{bmatrix} \quad (2)$$

From the above equation, it is clear that by using data diversity and space-time coding technique in transmitting and receiving ends, the best performance of the wireless communication system can be achieved.

III. CHANNEL ESTIMATION ALGORITHMS

For the k^{th} sub-carrier, $H_{ij}(k)$ is the frequency-domain channel response function for the i^{th} receive antenna and the j^{th} transmit antenna. $\boldsymbol{H}$ is the channel response in time-domain. For a 20MHz bandwidth, there are 64 sub-carriers. Thus, $k = 0, 1, 2, \ldots\ldots, 63$ and sub-carrier spacing is 312.5kHz.

A. Maximum Likelihood (ML) Algorithm

After OFDM demodulation, the receive signal is shown as

$$r_i(k) = H_{ij}(k) s_j(k) + n_i(k) \quad (3)$$

where $s_j(k)$ is the j^{th} transmit training signal, $r_j(k)$ is the i^{th} receive signal and $n_j(k)$ is the i^{th} receive noise. If the noise is Gaussian, the channel estimation is shown as

$$H_{ij}(k) \approx \hat{H}_{ij}(k) = \frac{r_i(k)}{s_j(k)} \quad (4)$$

Since $s_j(k)$ is non-zero for only 56 sub-carriers (k = 1~28, 36~63), the others 8 sub-carriers (k = 0, 29~35) are null.

B. Time-Domain Truncation (TDT) Approach

It derives the channel impulse response (CIR) by applying the IFFT on these transfer functions. It truncates the impulse response to remove weak and noise late arrivals in the time-domain. Finally, it performs FFT on the truncated channel response to yield an improved estimation of the channel transfer function in the frequency-domain. The method is called the time-domain truncation method (TDT) [5]. The TDT method works well for channels with short delay spreads. However, it requires initial channel estimation for all sub-carriers. It can get the accurate time-domain response by using time-domain and frequency-domain transform and L. [6]

The TDT algorithm consists of the following four steps:

Step I：

Using ML algorithm can obtain the initial estimation of the channel transfer functions for all sub-carries. Then, applying the IFFT can follow that

$$h_{ij}(l) = \frac{1}{N}\sum_{k=0}^{63} \hat{H}_{ij}(k) e^{\frac{j2\pi kl}{64}} \quad (5)$$

Since the channel transfer function has null sub-carriers, the time-domain channel response is approximated as

$$h_{ij}(l) \approx \hat{h}_{ij}(l) = \frac{1}{N}\sum_{K=1}^{28}\sum_{K=36}^{63} \hat{H}_{ij}(K) e^{\frac{j2\pi kl}{64}} \quad (6)$$

Step II：

Mainly decide the L value in this step, where L is the number of taps. There are many ways to determine L. After L is determined, we can express the tap coefficients of the CIR in terms of the estimated channel transfer functions as

$$H_{ij}(k) \approx \hat{H}_{ij}(k) = \sum_{l=0}^{63} h_{ij}(l) e^{\frac{-j2\pi kl}{64}} \approx \sum_{l=0}^{L-1} h_{ij}(l) e^{\frac{-j2\pi kl}{64}} \quad (7)$$

Step III：

In this step, an improved time-domain channel response is obtained. The response is zero when l is bigger than L. When l is smaller than L, we take its response value. It shows as

$$\tilde{h}_{ij}(l) = \begin{cases} \hat{h}_{ij}(l), & l < L \\ 0, & l \geq L \end{cases} \quad (8)$$

Step IV：

The improved channel transfer functions are obtained by performing FFT on the improved CIR as given by

$$H_{ij}(k) \approx \tilde{H}_{ij}(k) = \sum_{l=0}^{L-1} \tilde{h}_{ij}(l) e^{\frac{-j2\pi kl}{64}} \quad (9)$$

C. Space Time Block Code (STBC)

Under STBC construction, the channel environment is assumed to be the flat fading channel because STBC technology can only work in this environment. Along with present communication system, bandwidth increase and symbol cycle lessening, may lead to multipath effect because of channel transmission delay. Moreover, the multipath effect may cause frequency-selective fading channel. In this channel, inter symbol interference (ISI) is able to destroy the orthogonality of STBC. The application will therefore be limited in indoor short spread delay environment or low data-rate systems. By the combination of OFDM and STBC system and with OFDM, the bandwidth can be divided into many sub-carrier transmission signals. Hence, the frequency-selective fading channel can be regarded as many flat sub-channels combinations and STBC technology can be used to improve the performance of wireless communication system.

Fig. 1 shows a general architecture of STBC channel estimation and signal detection in OFDM system. For channel estimation, we first use training symbols for encoding on transmitting end and then divide them into multi-paths for IFFT and finally send them out with multi antennas. Two receiving antennas will then receive the signals, passing through FFT, and send them to the STBC decoder. The channel is therefore being detected.

Fig. 2 is a conventional channel estimation structure. It mainly distributes multi-paths into the pilot symbols or the preamble symbols of signal data in transmitting baseband, so as to estimate the frequency response of baseband. In this work, preamble symbols are used to obtain corresponding frequency response. Furthermore, with first or second order linear interpolation [7], we can obtain the frequency response of null preamble symbols.

Fig. 3 shows the preamble symbol signals of transmission, passing through STBC encoder. The signals are then transmitted by two transmission antennas and passed through the channel. After receiving by two receiving antennas and combining with the original transmitting preamble symbol signals, the channel response is estimated.

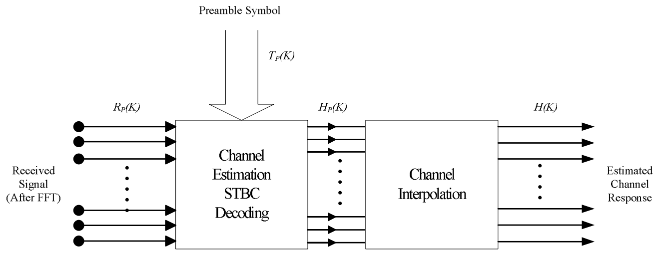

Figure 2. The block diagram of channel estimation

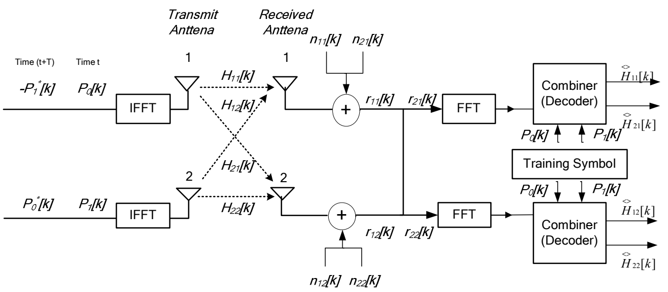

Figure 3. The channel estimation with preamble symbol

The channel response can be derived from Eqs. (10), (11), (12), and (13):

$$\hat{H}_{11}[k] = \frac{P_0^*[k]r_{11}[k] - P_1[k]r_{21}[k]}{|P_0[k]|^2 + |P_1[k]|^2} = H_{11}[k] + \frac{P_0^*[k]n_{11}[k] - P_1[k]n_{21}[k]}{|P_0[k]|^2 + |P_1[k]|^2} \quad (10)$$

$$\hat{H}_{21}[k] = \frac{P_1^*[k]r_{11}[k] + P_0[k]r_{21}[k]}{|P_0[k]|^2 + |P_1[k]|^2} = H_{21}[k] + \frac{P_1^*[k]n_{11}[k] + P_0[k]n_{21}[k]}{|P_0[k]|^2 + |P_1[k]|^2} \quad (11)$$

$$\hat{H}_{12}[k] = \frac{P_0^*[k]r_{12}[k] - P_1[k]r_{22}[k]}{|P_0[k]|^2 + |P_1[k]|^2} = H_{12}[k] + \frac{P_0^*[k]n_{12}[k] - P_1[k]n_{22}[k]}{|P_0[k]|^2 + |P_1[k]|^2} \quad (12)$$

$$\hat{H}_{22}[k] = \frac{P_1^*[k]r_{12}[k] + P_0[k]r_{22}[k]}{|P_0[k]|^2 + |P_1[k]|^2} = H_{22}[k] + \frac{P_1^*[k]n_{12}[k] + P_0[k]n_{22}[k]}{|P_0[k]|^2 + |P_1[k]|^2} \quad (13)$$

IV. SIMULATION RESULTS

Fig. 4 compares BER of our four algorithms in TGn B channel [8], [9]. When SNR is less than 20dB, there are no much difference between the performances of the four BERs. From the above three algorithms that we have mentioned, their SNR must be greater than 30dB, so as to make BER less than thousandth. However, from the derived TDT-L-STBC algorithm, BER is already lower than thousandth when SNR is 25dB. Therefore, we can still implement our hardware structure with a SNR drop of 5dB. Furthermore, when SNR is 30dB, BER can even be decreased to ten thousandth. Hence, it illustrates the superiority of TDT-L-STBC algorithm.

Fig. 5 shows the comparison of BER of our four algorithms in TGn D channel. The performances of the four BERs have no much difference when SNR is less than 20dB. In this channel, because of the greater delay diffusion, the BER performance will be worse. When SNR is 30dB, the performance of the TDT-L-STBC algorithm has no much difference compared with that in TGn B channel. However, smaller SNR can't make BER reach thousandth. Nevertheless, we can still see that our performance of the TDT-L-STBC algorithm is better than that of the other algorithms.

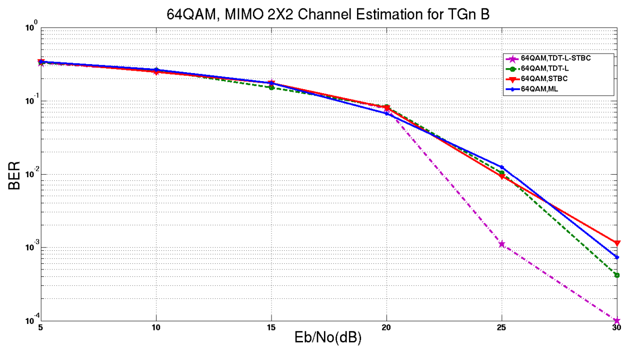

Figure 4. BER performance of four algorithms in TGn B channel

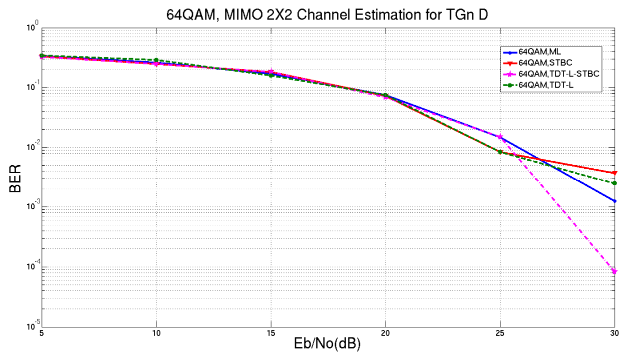

Figure 5. BER performance of four algorithms in TGn D channel

V. IMPLEMENTATION RESULTS

The architecture adopts 2×2 64-QAM MIMO system. The proposed architecture has three parts as shown in Fig. 6 i and j are the numbers of transmitting and receiving antennas, respectively, where $i = j = 2$. P is preamble symbol for channel estimation. n is noise signal. The proposed architecture to get the channel response matrix is using the transformation of frequency domain–time domain, then correction with STBC.

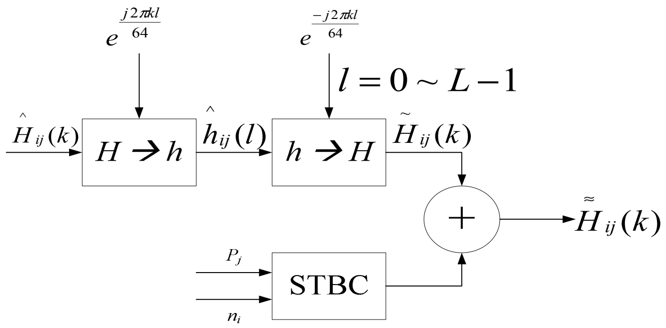

Figure 6. The architecture of TDT-L-STBC

Table I shows the comparison of the performance between TDT-L and TDT-L-STBC algorithms. TDT-L with STBC consumes more hardware area, but the performance of BER becomes better. In this way, BER can be raised more than 3dB.

TABLE I. PERFORMANCE COMPARISON OF TDT-L AND TDT-L-STBC ALGORITHMS

Reference	TDT-L	TDT-L-STBC
Technology	TSMC 0.18μm	TSMC 0.18μm
Antenna Pair	2×2	2×2
Modulation Type	64-QAM	64-QAM
Max. CLK Freq.(MHz)	62.5	50
Area(mm^2)	3.56	3.88
Equivalent Gate Count	355.5K	387.6K
Power (mW)	48.0	52.9
SNR(dB): BER@10^{-3} for TGn B channel	28.6	25.1
SNR(dB): BER@10^{-3} for TGn B channel	N/A	27.7

From Table II and Table III, we can know the difference between the proposed work and Ref. [10]. The greatest operating frequency in this work is smaller than that in [10]. However, it's not a serious problem because the proposed work is designed directly for IEEE802.11n. It meets the specifications as long as the frequency is above 40MHz. The proposed hardware is better than [10] both in area and power consumption. Moreover, we are using MIMO-2x2 while [10] is using MIMO-4x4. Therefore, the number of antennas is saved.

TABLE II. PERFORMANCE COMPARISON OF HARDWARE

Reference	Ref. [10]	This work
Technology	UMC 0.13μm	TSMC 0.18μm
Antenna Pair	4×4	2×2
Modulation Type	QPSK	64-QAM
Max. CLK Freq.(MHz)	101	50
Area(mm^2)	3.25	3.88
Equivalent Gate Count	638.2K	387.6K
Power (mW)	84.5	52.9

TABLE III. PERFORMANCE COMPARISON OF FPGA XILINX HARDWARE

Reference	Ref. [10]			This work		
Technology	Xilinx Virtex-II Pro			Xilinx Virtex-V Pro		
Max. CLK Freq.	48.7 MHz			54.1 MHz		
Resource	Used	Available	Percentage	Used	Available	Percentage
Slices	1304	13696	9%	3461	103680	3%
Slices FF	947	27392	3%	422	207360	0%
LUTs	2442	27392	8%	3497	207360	2%
IOs	56			117		
Bound IOBs	56	556	10%	117	1200	1%

VI. CONCLUSION

This paper presents the channel estimation for MIMO-OFDM systems in a wireless baseband receiver and is designed directly for IEEE802.11n, with a combined channel estimation algorithm, TDT-L-STBC. This work is implemented with TSMC 0.18um CMOS technology. Compared with the conventional channel estimation algorithm, the proposed work consumes a little more hardware area but the performance of BER is improved. Moreover, by using MIMO-2x2, the number of antennas is saved. The maximum CLK frequency is 40 MHz, the area is $3.88mm^2$ and the power consumption is 52.9mW.

ACKNOWLEDGMENT

This work was supported in part by the National Science Council (NSC), Taiwan, R. O. C. under grant NSC 99-2221-E-005-110 and NSC 99-2221-E-167-033 and in part by the ministry of education, Taiwan, R. O. C. under the ATU plan. The authors would like to thank the National Chip Implementation Center (CIC) of Taiwan for technical support.

REFERENCES

[1] Y.-H. Chung and S.-M. Phoong, "Joint estimation of I/Q imbalance, CFO and channel response for MIMO OFDM systems," *IEEE Trans. Commun.*, vol. 58, no. 5, pp. 1485-1492, May 2010.

[2] R. C. Chang, C.-H. Lin, K.-H. Lin, C.-L. Huang, and F.-C. Chen, "Iterative QR decomposition architecture using the modified Gram-Schmidt algorithm for MIMO systems," *IEEE Trans. Circuits Systems I: Regular papers*, vol. 57, no. 5, pp. 1095-1102, May 2010.

[3] V. Tarokh, H. Jafarkhani, and A. R. Calderbank, "Space-time block codes from orthogonal designs," *IEEE Trans. on Inform. Theory*, vol. 45, no. 7, pp. 1456-1467, Jul. 1999.

[4] V. Tarokh, N. Seshadri, and A. R. Calderbank, "Space-time codes for high data rate wireless communication: performance criteria and code construction," *IEEE Trans. on Inform. Theory*, vol. 44, no. 2, pp. 744-765, Mar. 1998.

[5] I-T. Lu, K.-J. Tsai, " Channel estimation in a proposed IEEE802.11n OFDM MIMO WLAN system," in *Proc. 2007 IEEE Sarnoff Symposium*, Jul. 2007, pp.1-5.

[6] V. D. Nguyen, H. Kuchenbecker, and M. Patzold, "Estimation of the channel impulse response length and the noise variance for OFDM systems," in *Proc. IEEE Vehicular Technology Conf.*, Dec. 2005, vol. 1, pp. 429-433.

[7] W. G. Jeon, K. H. Paik, and Y. S. Cho, "An efficient channel estimation technique for OFDM systems with transmitter diversity," *IEEE Int. Symp. Personal, Indoor Mobile Radio Commun.*, vol. 2, pp. 1246-1250, Aug. 2000.

[8] V. Erceg, et al., "IEEE P802.11 Wireless LANs: TGn Channel Models," *IEEE 802.11-03/940r4*, May 2004.

[9] S. A. Mujtaba, "TGn Sync Proposal Technical Specification," *IEEE802.11-04/889r4*, June 2005.

[10] M. Diallo, L. Boher, R. Rabineau, L. Cariou and M. Hélard, "Transform domain channel estimation with null subcarriers for MIMO-OFDM systems," in *Proc. IEEE International Symposium on Wireless Communication Systems*, Oct. 2008, pp. 209-213.